

Chapter 1

Fat-tailed variational inference

In some applications of probabilistic modeling, researchers may desire to explicitly model large deviation “tail” or “black-swan” events. While fat-tailed densities commonly arise as posterior and marginal distributions in robust models and scale mixtures, they present challenges when prior methods (including ??) fails to capture tail decay accurately. In this chapter, we first improve previous theory on tails of Lipschitz flows by quantifying how the tails affect the *rate* of tail decay and by expanding the theory to non-Lipschitz polynomial flows. We then develop an alternative theory for multivariate tail parameters which is sensitive to tail-anisotropy. In doing so, we unveil a fundamental problem which plagues many existing flow-based methods: they can only model tail-isotropic distributions (i.e., distributions having the same tail parameter in every direction). To mitigate this and enable modeling of tail-anisotropic targets, we propose anisotropic tail-adaptive flows (ATAF). Experimental results on both synthetic and real-world targets confirm that ATAF is competitive with prior work while also exhibiting appropriate tail-anisotropy. Parts of this chapter were first presented in Feynman Liang, Liam Hodgkinson, and Michael Mahoney. “Fat-Tailed Variational Inference with Anisotropic Tail Adaptive Flows”. In: *Proceedings of the 39th International Conference on Machine Learning*. Vol. 162. 2022, p. 132.

1.1 Introduction

Flow-based methods [Pap+21] have proven to be effective techniques to model complex probability densities. They compete with the state of the art on density estimation [Hua+18; Dur+19; Jai+20], generative modeling [Che+19; KD18], and variational inference [Kin+16; ASD20] tasks. These methods start with a random variable X having a simple and tractable distribution μ , and then apply a learnable transport map f_θ to build another random variable $Y = f_\theta(X)$ with a more expressive *pushforward* probability measure $(f_\theta)_*\mu$ [Pap+21]. In contrast to the implicit distributions [Hus17] produced by generative adversarial networks (GANs), flow-based methods restrict the transport map f_θ to be invertible and to have efficiently-computable Jacobian determinants. As a result, probability density functions can

be tractably computed through direct application of a change of variables

$$p_Y(y) = p_X(f_\theta^{-1}(y)) \left| \det \frac{df_\theta^{-1}(z)}{dz} \right|_{z=y}. \quad (1.1)$$

While recent developments [Che+19; Hua+18; Dur+19] have focused primarily on the transport map f_θ , the base distribution μ has received comparatively less investigation. The most common choice for the base distribution is standard Gaussian $\mu = \mathcal{N}(0, \mathbf{I})$. However, in Theorem 1.1, we show this choice results in significant restrictions on the expressivity of the model, limiting its utility for data that exhibits fat-tailed (or heavy-tailed) structure. Prior work addressing heavy-tailed flows [Jai+20] are limited to tail-isotropic base distributions. In Proposition 1.1, we prove flows built on these base distributions are unable to model accurately multivariate anisotropic fat-tailed structure.

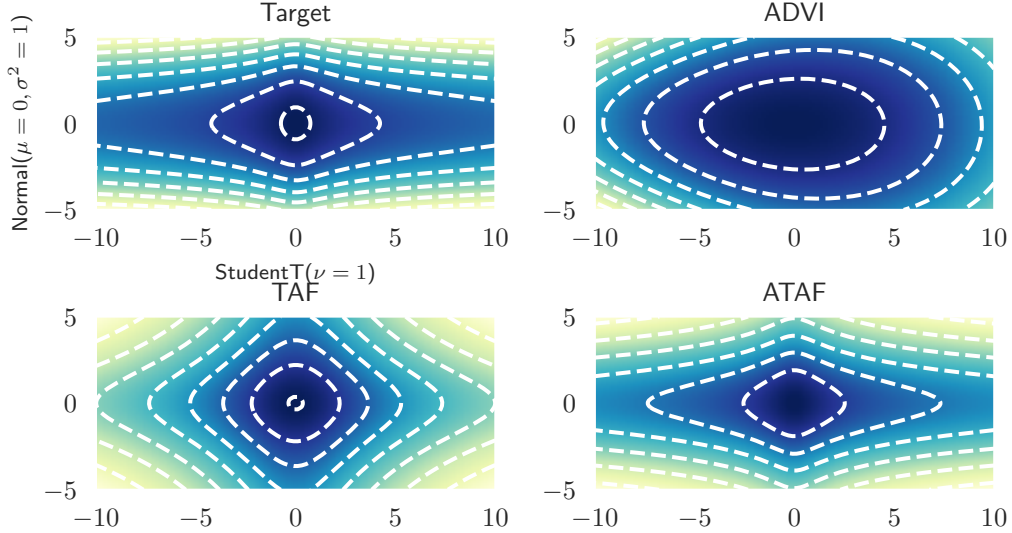


Figure 1.1: Variational inference against a tail-anisotropic target distribution $\mathcal{N}(0, 1) \otimes \text{StudentT}(\nu = 1)$ (top left). Only ATAF (bottom right) is able to correctly reproduce the tail-anisotropy (fat-tailed along x -axis, Gaussian along y -axis). In contrast, ADVI’s (top right) Gaussian base distribution and TAF’s (bottom left) tail-isotropic $\prod_{i=1}^2 \text{StudentT}(\nu)$ base distribution can only model tail-isotropic distributions (Proposition 1.1), which erroneously imposes power-law tails with the same rate of decay along both the x and y axes.

Our work here aims to identify and address these deficiencies. To understand the impact of the base distribution μ in flow-based models, we develop and apply theory for fat-tailed random variables and their transformations under Lipschitz-continuous functions. Our approach leverages the theory of concentration functions [Led01, Chapter 1.2] to sharpen significantly and extend prior results [JSY19, Theorem 4] by describing precisely the tail parameters

of the pushforward distribution $(f_\theta)_*\mu$ under both Lipschitz-continuous (Theorem 1.1) and polynomial (Corollary 1.2) transport maps. In the multivariate setting, we develop a theory of direction-dependent tail parameters (Definition 1.4), and we show that tail-isotropic base distributions yield tail-isotropic pushforward measures (Proposition 1.1). As a consequence of Proposition 1.1, prior methods [Jai+20] are limited in that they are unable to capture *tail-anisotropy*. This motivates the construction of *anisotropic tail adaptive flows* (ATAF, Definition 1.5) as a means to alleviate this issue (Remark 1.1) and to improve modeling of tail-anisotropic distributions. Our experiments show that ATAF exhibits correct tail behaviour in synthetic target distributions exhibiting fat-tails (Figure 1.5 of Section 1.5) and tail-anisotropy (Figure 1.1). On realistic targets, we find that ATAF can yield improvements in variational inference (VI) by capturing potential tail-anisotropy (Section 1.4).

Related Work

Fat-Tails in Variational Inference. Recent work in variational autoencoders (VAEs) have considered relaxing Gaussian assumptions to heavier-tailed distributions [Mat+19; Che+19; Boe+20; AO20]. In Mathieu et al. [Mat+19], a StudentT prior distribution $p(z)$ is considered over the latent code z in a VAE with Gaussian encoder $q(z | x)$. They argue that the anisotropy of a StudentT product distribution leads to more disentangled representations, as compared to the standard choice of Normal distributions. A similar modification is performed in Chen et al. [CSN20] for a coupled VAE [Cao+22]. This result showed improvements in the marginal likelihoods of reconstructed images. In addition, Boenninghoff et al. [Boe+20] consider a mixture of StudentTs for the prior $p(z)$. To position our work in context, note that the encoder $q(z | x)$ may be viewed as a variational approximation to the posterior $p(z | x)$ defined by the decoder model $p(x | z)$ and the prior $p(z)$. Our work differs from Mathieu et al. [Mat+19], Chen et al. [CSN20], and Boenninghoff et al. [Boe+20], in that we consider fat-tailed variational approximations $q(z | x)$ rather than priors $p(z)$. Although Abiri et al. [AO20] also considers a StudentT approximate posterior, our work involves a more general variational family which uses normalizing flows. Similarly, although Wang et al. [WLL18] also deals with fat-tails in variational inference, their goal is to improve α -divergence VI by controlling the moments of importance sampling ratios (which may be heavy-tailed). Our work here adopts Kullback-Leibler divergence and is concerned with enriching the variational family to include anisotropic fat-tailed distributions. More directly comparable recent work [DQV11; FSS17] studies the t -exponential family variational approximation which includes StudentTs and other heavier-tailed densities. Critically, the selection of their parameter t (directly related to the StudentT’s degrees of freedom ν), and the issue of tail anisotropy, are not discussed.

Flow-Based Methods. Normalizing flows and other flow-based methods have a rich history within variational inference [Kin+16; RM15; ASD20; Web+19]. Consistent with our experience (Figure 1.6), Webb et al. [Web+19] documents normalizing flows can offer improvements over ADVI and NUTS across thirteen different Bayesian linear regression

models from Gelman et al. [GH06]. Agrawal et al. [ASD20] shows that normalizing flows compose nicely with other advances in black-box VI (e.g., stick the landing, importance weighting). However, none of these works treat the issue of fat-tailed targets and inappropriate tail decay. To our knowledge, only TAFs [Jai+20] explicitly consider flows with tails heavier than Gaussians. Our work here can be viewed as a direct improvement of Jaini et al. [Jai+20], and we make extensive comparison to this work throughout the body of this paper. At a high level, we provide a theory for fat-tails which is sensitive to the rate of tail decay and develop a framework to characterize and address the tail-isotropic limitations plaguing TAFs.

1.2 Flow-Based Methods for Fat-Tailed Variational Inference

Flow-Based VI Methods

The objective of VI is to approximate a target distribution $\pi(x)$ by searching over a *variational family* $\mathcal{Q} = \{q_\phi : \phi \in \Phi\}$ of probability distributions q_ϕ . While alternatives exist [LT16; WLL18], VI typically seeks to find q_ϕ “close” to π , as measured by Kullback-Leibler divergence $D(q_\phi \parallel \pi)$. To ensure tractability without sacrificing generality, in practice [WW13; RGB14] a Monte-Carlo approximation of the evidence lower bound (ELBO) is maximized:

$$\begin{aligned} \text{ELBO}(\phi) &= \int q_\phi(x) \log \frac{\bar{\pi}(x)}{q_\phi(x)} dx \\ &\approx \frac{1}{n} \sum_{i=1}^n \log \frac{\bar{\pi}(x_i)}{q_\phi(x_i)}, \quad x_i \stackrel{\text{i.i.d.}}{\sim} q_\phi, \quad \bar{\pi} \propto \pi. \end{aligned}$$

To summarize, this procedure enables tractable black-box VI by replacing π with $\bar{\pi} \propto \pi$ and approximating expectations with respect to q_ϕ (which are tractable only in simple variational families) through Monte-Carlo approximation. In Bayesian inference and probabilistic programming applications, the target posterior $\pi(x) = p(x \mid y) = \frac{p(x,y)}{p(y)}$ is typically intractable but $\bar{\pi}(x) = p(x, y)$ is computable (i.e., represented by the probabilistic program’s generative / forward execution).

While it is possible to construct a variational family \mathcal{Q} tailored to a specific task, we are interested in VI methods which are more broadly applicable and convenient to use: \mathcal{Q} should be automatically constructed from introspection of a given probabilistic model/program. Automatic differentiation variational inference (ADVI, Kucukelbir et al. [Kuc+17]) is an early implementation of automatic VI and it is still the default in certain probabilistic programming languages [Car+17]. ADVI uses a Gaussian base distribution μ and a transport map $f_\theta = f \circ \Phi_{\text{Affine}}$ comprised of an invertible affine transform composed with a deterministic transformation f from \mathbb{R} to the target distribution’s support (e.g., $\exp : \mathbb{R} \rightarrow \mathbb{R}_{\geq 0}$, $\text{sigmoid} : \mathbb{R} \rightarrow [0, 1]$). As Gaussians are closed under affine transformations, ADVI’s representational capacity is limited to deterministic transformations of Gaussians. Hence it cannot represent

Model	Autoregressive transform	Suff. cond. for Lipschitz-continuity
NICE[DKB15]	$z_j + \mu_j \cdot \mathbb{1}_{k \notin [j]}$	μ_j Lipschitz
MAF[PPM17]	$\sigma_j z_j + (1 - \sigma_j) \mu_j$	σ_j bounded
IAF[Kin+16]	$z_j \cdot \exp(\lambda_j) + \mu_j$	λ_j bounded, μ_j Lipschitz
Real-NVP[DSB17]	$\exp(\lambda_j \cdot \mathbb{1}_{k \notin [j]}) \cdot z_j + \mu_j \cdot \mathbb{1}_{k \notin [j]}$	λ_j bounded, μ_j Lipschitz
Glow[KD18]	$\sigma_j \cdot z_j + \mu_j \cdot \mathbb{1}_{k \notin [j]}$	σ_j bounded, μ_j Lipschitz
NAF[Hua+18]	$\sigma^{-1}(w^\top \cdot \sigma(\sigma_j z_j + \mu_j))$	Always (logistic mixture CDF)
NSF[Dur+19]	$z_j \mathbb{1}_{z_j \notin [-B, B]} + M_j(z_j; z_{< j}) \mathbb{1}_{x_j \in [-B, B]}$	Always (linear outside $[-B, B]$)
FFJORD[Gra+19]	n/a (not autoregressive)	Always (required for invertibility)
ResFlow[Che+19]	n/a (not autoregressive)	Always (required for invertibility)

Table 1.1: Some popular / recently developed flows, the autoregressive transform used in the flow (if applicable), and sufficient conditions for Lipschitz-continuity. A subset of this table was first presented in Jaini et al. [Jai+20]. $M(\cdot)$ denotes monotonic rational quadratic splines [Dur+19].

complex multi-modal distributions. To address this, more recent work [Kin+16; Web+19] replaces the affine map Φ_{Affine} with a flow Φ_{Flow} typically parameterized by an invertible neural network:

Definition 1.1 *ADVI (with normalizing flows) comprise the variational family $\mathcal{Q}_{\text{ADVI}} := \{(f \circ \Phi_{\text{Flow}})_* \mu\}$, where $\mu = \text{Normal}(0_d, I_d)$, Φ_{Flow} is an invertible flow transform (e.g., Table 1.1) and f is a deterministic bijection between constrained supports [Kuc+17].*

As first noted in Jaini et al. [Jai+20], the pushforward of a light-tailed Gaussian base distribution under a Lipschitz-continuous flow will remain light-tailed and provide poor approximation to fat-tailed targets. Despite this, many major probabilistic programming packages still make a default choice of Gaussian base distribution (`AutoNormalizingFlow`/`AutoIAFNormal` in Pyro [Bin+19], `method=variational` in Stan [Car+17], `NormalizingFlowGroup` in PyMC [PHF10]). To address this issue, tail-adaptive flows [Jai+20] use a base distribution $\mu_\nu = \prod_{i=1}^d \text{StudentT}(\nu)$, where a single degrees-of-freedom $\nu \in \mathbb{R}$ is used across all d dimensions. Here is a more precise definition.

Definition 1.2 *Tail adaptive flows (TAF) comprise the variational family $\mathcal{Q}_{\text{TAF}} := \{(f \circ \Phi_{\text{Flow}})_* \mu_\nu\}$, where $\mu_\nu = \prod_{i=1}^d \text{StudentT}(\nu)$ with ν shared across all d dimensions, Φ_{Flow} is an invertible flow, and f is a bijection between constrained supports [Kuc+17]. During training, the shared degrees of freedom ν is treated as an additional variational parameter.*

Fat-Tailed Variational Inference

Fat-tailed variational inference (FTVI) considers the setting where the target $\pi(x)$ is fat-tailed. Such distributions commonly arise during a standard “robustification” approach where light-tailed noise distributions are replaced with fat-tailed ones [TL05]. They also appear when weakly informative prior distributions are used in Bayesian hierarchical models [Gel+06].

To formalize these notions of fat-tailed versus light-tailed distributions, a quantitative classification for tails is required. While prior work classified distribution tails according to quantiles and the existence of moment generating functions [Jai+20, Section 3], here we propose a more natural and finer-grained classification based upon the theory of concentration functions [Led01, Chapter 1.2], which is sensitive to the rate of tail decay.

Definition 1.3 (Classification of tails) *For each $\alpha, p > 0$, we let*

- \mathcal{E}_α^p *denote the set of exponential-type random variables X with $\mathbb{P}(|X| \geq x) = \Theta(e^{-\alpha x^p})$;*
- \mathcal{L}_α^p *denote the set of logarithmic-type random variables X with $\mathbb{P}(|X| \geq x) = \Theta(e^{-\alpha(\log x)^p})$.*

In both cases, we call p the class index and α the tail parameter for X . Note that every \mathcal{E}_α^p and \mathcal{L}_β^q are disjoint, that is, $\mathcal{E}_\alpha^p \cap \mathcal{L}_\beta^q = \emptyset$ for all $\alpha, \beta, p, q > 0$. For brevity, we define the ascending families $\overline{\mathcal{E}}_\alpha^p$ and $\overline{\mathcal{L}}_\alpha^p$ analogously as before except with $\Theta(\cdot)$ replaced by $\mathcal{O}(\cdot)$. Similarly, we denote the class of distributions with exponential-type tails with class index at least p by $\overline{\mathcal{E}}^p = \cup_{\alpha \in \mathbb{R}_+} \mathcal{E}_\alpha^p$, and similarly for $\overline{\mathcal{L}}^p$.

For example, $\overline{\mathcal{E}}_\alpha^2$ corresponds to $\alpha^{-1/2}$ -sub-Gaussian random variables, $\overline{\mathcal{E}}_\alpha^1$ corresponds to sub-exponentials, and (of particular relevance to this paper) \mathcal{L}_α^1 corresponds to the class of power-law distributions.

1.3 Tail Behavior of Lipschitz Flows

This section contains our main theoretical contributions and proofs. We sharpen previous impossibility results approximating fat-tailed targets using light-tailed base distributions [Jai+20, Theorem 4] by characterizing the effects of Lipschitz-continuous transport maps on not only the tail class but also the class index and tail parameter (Definition 1.3). Furthermore, we extend the theory to include polynomial flows [JSY19]. For the multivariate setting, we define the tail-parameter function (Definition 1.4) to help formalize the notion of tail-isotropic distributions and prove a fundamental limitation that tail-isotropic pushforwards remain tail-isotropic (Proposition 1.1).

As an initial but nevertheless crucial result, we first bound the tail parameters of the sum of two power law random variables.

Lemma 1.1 *Suppose $X \in \mathcal{L}_\alpha^1$ and $Y \in \mathcal{L}_\beta^1$. Then $X + Y \in \mathcal{L}_{\min\{\alpha, \beta\}}^1$.*

Proof First, let $\gamma = \min\{\alpha, \beta\}$. It will suffice to show that (I) $\mathbb{P}(|X + Y| \geq r) = \mathcal{O}(r^{-\gamma})$, and (II) $\mathbb{P}(|X + Y| \geq r) \geq \Theta(r^{-\gamma})$. Since $(X, Y) \mapsto |X + Y|$ is a 1-Lipschitz function on \mathbb{R}^2 and $\mathbb{P}(|X| \geq r) + \mathbb{P}(|Y| \geq r) = \mathcal{O}(r^{-\gamma})$, (I) follows directly from the hypotheses and Proposition 1.11 of Ledoux [Led01]. To show (II), note that for any $M > 0$, conditioning on the event $|Y| \leq M$,

$$\mathbb{P}(|X| + |Y| \geq r \mid |Y| \leq M) \geq \mathbb{P}(|X| \geq r - M).$$

Therefore, by taking M to be sufficiently large so that $\mathbb{P}(|Y| \leq M) \geq \frac{1}{2}$,

$$\begin{aligned} \mathbb{P}(|X + Y| \geq r) &\geq \mathbb{P}(|X| + |Y| \geq r) \\ &\geq \mathbb{P}(|X| + |Y| \geq r \mid |Y| \leq M) \mathbb{P}(|Y| \leq M) \\ &\geq \frac{1}{2} \mathbb{P}(|X| \geq r - M) = \Theta(r^{-\alpha}). \end{aligned}$$

The same process with X and Y reversed implies $\mathbb{P}(|X + Y| \geq r) \geq \Theta(r^{-\beta})$ as well. Both (II) and the claim follow. \blacksquare

Most of our following results are developed within the context of Lipschitz-continuous transport maps f_θ . In practice, many flow-based methods exhibit Lipschitz-continuity in their transport map, either by design [Gra+19; Che+19], or as a consequence of choice of architecture and activation function (Table 1.1). The following assumption encapsulates this premise.

Assumption 1.1 *f_θ is invertible, and both f_θ and f_θ^{-1} are L -Lipschitz continuous (e.g., sufficient conditions in Table 1.1 are satisfied).*

It is worth noting that domains other than \mathbb{R}^d may require an additional bijection between supports (e.g. $\exp : \mathbb{R} \rightarrow \mathbb{R}_+$) which could violate assumption 1.1.

Closure of Tail Classes

Our first set of results pertains to the closure of the tail classes in Definition 1.3 under Lipschitz-continuous transport maps. While earlier work [Jai+20] demonstrated closure of exponential-type distributions $\cup_{p>0} \overline{\mathcal{E}^p}$ under flows satisfying Assumption 1.1, our results in Theorem 1.1 and Corollaries 1.1 and 1.2 sharpen these observations, showing that: (1) Lipschitz transport maps cannot decrease the class index p for exponential-type random variables, but they can alter the tail parameter α ; and (2) under additional assumptions, they cannot change either class index p or the tail parameter α for logarithmic-type random variables.

Theorem 1.1 (Lipschitz maps of tail classes) *Under Assumption 1.1, the distribution classes $\overline{\mathcal{E}^p}$ and $\overline{\mathcal{L}_\alpha^p}$ (with $p, \alpha > 0$) are closed under every flow transformation in Table 1.1.*

Informally, Theorem 1.1 asserts that light-tailed base distributions cannot be transformed via Lipschitz transport maps into fat-tailed target distributions. Note this does not violate universality theorems for certain flows [Hua+18] as these results only apply in the infinite-dimensional limit. Indeed, certain exponential-type families (such as Gaussian mixtures) are dense in the class of *all* distributions, including those that are fat-tailed.

Proof [Proof of Theorem 1.1] Let X be a random variable from either \mathcal{E}_α^p or \mathcal{L}_α^p . Its concentration function (Equation 1.6 Ledoux [Led01]) is given by

$$\alpha_X(r) := \sup\{\mu\{x : d(x, A) \geq r\}; A \subset \text{supp } X, \mu(A) \geq 1/2\} = \mathbb{P}(|X - m_X| \geq r).$$

Under Assumption 1, f_θ is Lipschitz (say with Lipschitz constant L) so by Proposition 1.3 of Ledoux [Led01],

$$\mathbb{P}(|f_\theta(X) - m_{f_\theta(X)}| \geq r) \leq 2\alpha_X(r/L) = \mathcal{O}(\alpha_X(r/L)),$$

where $m_{f_\theta(X)}$ is a median of $f_\theta(X)$. Furthermore, by the triangle inequality

$$\begin{aligned} \mathbb{P}(|f_\theta(X)| \geq r) &= \mathbb{P}(|f_\theta(X) - m_{f_\theta(X)} + m_{f_\theta(X)}| \geq r) \\ &\leq \mathbb{P}(|f_\theta(X) - m_{f_\theta(X)}| \geq r - |m_{f_\theta(X)}|) \\ &= \mathcal{O}(\mathbb{P}(|f_\theta(X) - m_{f_\theta(X)}| \geq r)) \\ &= \mathcal{O}(\alpha_X(r/L)), \end{aligned} \tag{1.2}$$

where the asymptotic equivalence holds because $|m_{f_\theta(X)}|$ is independent of r . When $X \in \mathcal{E}_\alpha^p$, Equation (1.2) implies

$$\mathbb{P}(|f_\theta(X)| \geq r) = \mathcal{O}(e^{-\frac{\alpha}{L}r^p}) \implies f_\theta(X) \in \overline{\mathcal{E}}_{\alpha/L}^p,$$

from whence we find that the Lipschitz transform of exponential-type tails continues to possess exponential-type tails with the same class index p , although the tail parameter may have changed. Hence, $\overline{\mathcal{E}}^p$ is closed under Lipschitz maps for each $p \in \mathbb{R}_{>0}$. On the other hand, when $X \in \mathcal{L}_\alpha^p$, Equation (1.2) also implies that

$$\mathbb{P}(|f_\theta(X)| \geq r) = \mathcal{O}(e^{-\alpha(\log(r/L))^p}) = \mathcal{O}(e^{-\alpha(\log r)^p}),$$

and therefore, $f_\theta(X) \in \overline{\mathcal{L}}_\alpha^p$. Unlike exponential-type tails, Lipschitz transforms of logarithmic-type tails not only remain logarithmic, but their tails decay no slower than a logarithmic-type tail of the same class index with the *same* tail parameter α . This upper bound suffices to show closure under Lipschitz maps for the ascending family $\overline{\mathcal{L}}_\alpha^p$. ■

Note that $\overline{\mathcal{L}}_\alpha^p \supset \mathcal{E}_\beta^q$ for all p, q, α, β , so Theorem 1.1 by itself does not preclude transformations of fat-tailed base distributions to light-tailed targets. Under additional assumptions on f_θ , we further establish a partial converse that a fat-tailed base distribution's tail parameter is unaffected after pushforward, hence heavy-to-light transformations are impossible. Note here there is no ascending union over tail parameters (i.e., \mathcal{L}_α^p instead of $\overline{\mathcal{L}}_\alpha^p$).

Corollary 1.1 (Closure of \mathcal{L}_α^p) *If in addition f_θ is smooth with no critical points on the interior or boundary of its domain, then \mathcal{L}_α^p is closed.*

This implies that simply fixing a fat-tailed base distribution *a priori* is insufficient; the tail-parameter(s) of the base distribution must be explicitly optimized alongside the other variational parameters during training. While these additional assumptions may seem restrictive, note that many flow transforms explicitly enforce smoothness and monotonicity [WL19; Hua+18; Dur+19] and hence satisfy the premises.

Proof [Proof of Corollary 1.1] Let f_θ be as before with the additional assumptions. Since f_θ is a smooth continuous bijection, it is a diffeomorphism. Furthermore, by assumption f_θ has invertible Jacobian on the closure of its domain hence $\sup_{x \in \text{dom } f_\theta} |(f_\theta)'(x)| \geq M > 0$. By the inverse function theorem, $(f_\theta)^{-1}$ exists and is a diffeomorphism with

$$\frac{d}{dx}(f_\theta)^{-1}(x) = \frac{1}{(f_\theta)'((f_\theta)^{-1}(x))} \leq \frac{1}{M}.$$

Therefore, $(f_\theta)^{-1}$ is M^{-1} -Lipschitz and we may apply Theorem 1.1 to conclude the desired result. ■

In fact, we can show a version of Theorem 1.1 ensuring closure of exponential-type distributions under polynomial transport maps which do not satisfy Assumption 1.1. This is significant because it extends the closure results to include polynomial flows such as sum-of-squares flows [JSY19].

Corollary 1.2 (Closure under polynomial maps) *For any $\alpha, \beta, p, q \in \mathbb{R}_+$, there does not exist a finite-degree polynomial map from \mathcal{E}_α^p into \mathcal{L}_β^q .*

Proof [Proof of Corollary 1.2] Let $X \in \mathcal{E}_\alpha^p$. By considering sufficiently large X such that leading powers dominate, it suffices to consider monomials $Y = X^k$. Notice $\mathbb{P}(Y \geq x) = \mathbb{P}(X \geq x^{1/k}) = \Theta(e^{-\alpha x^{p/k}})$, and so $Y \in \mathcal{E}_\alpha^{p/k}$. The result follows by disjointness of \mathcal{E} and \mathcal{L} . ■

Multivariate Fat-Tails and Anisotropic Tail Adaptive Flows

Next, we restrict attention to power-law tails \mathcal{L}_α^1 , and we develop a multivariate fat-tailed theory and notions of isotropic/anisotropic tail indices. Using our theory, we prove that both ADVI and TAF are fundamentally limited because they are only capable of fitting tail-isotropic target measures (Proposition 1.1). We consider anisotropic tail adaptive flows (ATAF): a density modeling method which can represent tail-anisotropic distributions (Remark 1.1).

For example, consider the target distribution shown earlier in Figure 1.1 formed as the product of $\mathcal{N}(0, 1)$ and StudentT($\nu = 1$) distributions. The marginal/conditional distribution along a horizontal slice (e.g., the distribution of $\langle X, e_0 \rangle$) is fat-tailed, while along a vertical slice (e.g., $\langle X, e_1 \rangle$) it is Gaussian. Another extreme example of tail-anisotropy where the tail parameter for $\langle X, v \rangle$ is different in every direction $v \in \mathcal{S}^1$ is given in Figure 1.2. Here \mathcal{S}^{d-1} denotes the $(d-1)$ -sphere in d dimensions. Noting that the tail parameter depends on the

choice of direction, we are motivated to consider the following direction-dependent definition of multivariate tail parameters.

Definition 1.4 For a d -dimensional random vector X , its tail parameter function $\alpha_X : \mathcal{S}^{d-1} \rightarrow \mathbb{R}_+$ is defined as $\alpha_X(v) = -\lim_{x \rightarrow \infty} \log \mathbb{P}(\langle v, X \rangle \geq x) / \log x$ when the limit exists, and $\alpha_X(v) = +\infty$ otherwise. In other words, $\alpha_X(v)$ maps directions v into the tail parameter of the corresponding one-dimensional projection $\langle v, X \rangle$. The random vector X is tail-isotropic if $\alpha_X(v) \equiv c$ is constant and tail-anisotropic if $\alpha_X(v)$ is not constant but bounded.

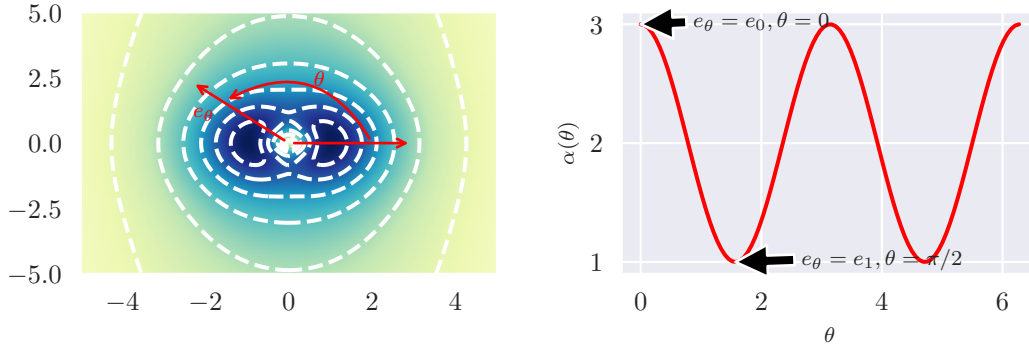


Figure 1.2: Illustration of the direction-dependent tail-parameter function (right) on a tail-anisotropic distribution (left) with PDF $dP(r, \theta) = r^{-\alpha(\theta)} r dr d\theta$ and tail parameter $\alpha(\theta) = 2 + \cos(2\theta)$. While prior fat-tailed theory based on $\|X\|_2 = \sup_{\|v\|_2=1} \langle X, v \rangle$ is only sensitive to the largest tail parameter $\max_{\theta \in [0, 2\pi]} \alpha(\theta) = 3.0$, our direction-dependent tail parameter function (bottom, red line) and its values along the standard basis axes ($\alpha(0)$ and $\alpha(\pi/2)$) capture *tail-anisotropy*.

Example of Non-existence of Tail Parameter Due to Oscillations

Of course, one can construct pathological densities where this definition is not effective. As a degenerate example, consider $\text{StudentT}(\nu = 1) \otimes \text{StudentT}(\nu = 2)$ and “spin” it using the radial transformation $(r, \theta) \mapsto (r, r + \theta)$ (Figure 1.3). Due to oscillations, $\alpha_X(v)$ is not well defined for all $v \in \mathcal{S}^1$.

Comparison versus TAF

It is illustrative to contrast with the theory presented for TAF [Jai+20], where only the tail exponent of $\|X\|_2$ is considered. For $X = (X_1, \dots, X_d)$ with $X_i \in \mathcal{L}_{\alpha_i}^1$, by Fatou-Lebesgue

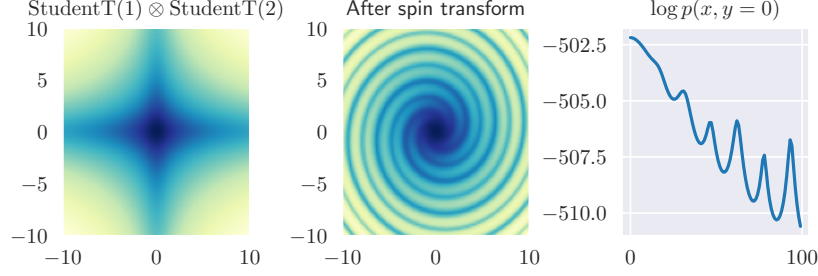


Figure 1.3: Taking a tail-anisotropic distribution (left) and “spinning” it (middle) results in one-dimensional projections which oscillate between tail parameters (as seen in $\log p(\langle X, e_0 \rangle)$ in right panel) and result in an ill-defined direction-dependent tail parameter function $\alpha_X(\cdot)$ due to a divergent limit.

and Lemma 1.1

$$\begin{aligned} \mathbb{P}[\|X\|_2 \geq t] &= \mathbb{P}\left[\sup_{z \in \mathcal{S}^{d-1}} \langle X, z \rangle \geq t\right] \\ &\geq \sup_{z \in \mathcal{S}^{d-1}} \mathbb{P}[\langle X, z \rangle \geq t] = \max_{1 \leq i \leq d} \nu_i = \max_{0 \leq i \leq d-1} \alpha_X(e_i). \end{aligned}$$

Therefore, considering only the tail exponent of $\|X\|_2$ is equivalent to summarizing $\alpha_X(\cdot)$ by an upper bound. Given the absence of the tail parameters for other directions (i.e., $\alpha_X(v) \neq \sup_{\|v\|=1} \alpha_X(v)$) in the theory for TAF [Jai+20], it should be unsurprising that both their multivariate theory as well as their experiments only consider tail-isotropic distributions obtained either as an elliptically-contoured distribution with fat-tailed radial distribution or $\prod_{i=1}^d \text{StudentT}(\nu)$ (tail-isotropic by Lemma 1.1). Our next proposition shows that this presents a significant limitation when the target distribution is tail-anisotropic.

Proposition 1.1 (Pushforwards of tail-isotropic distributions) *Let μ be tail isotropic with non-integer parameter ν and suppose f_θ satisfies Assumption 1.1. Then $(f_\theta)_*\mu$ is tail isotropic with parameter ν .*

To show Proposition 1.1, we will require a few extra assumptions to rule out pathological cases. The full content of Proposition 1.1 is contained in the following theorem.

Theorem 1.2 *Suppose there exists $\nu > 0$ such that $C : \mathcal{S}^{d-1} \rightarrow (0, \infty)$ satisfies $C(v) := \lim_{x \rightarrow \infty} x^\nu \mathbb{P}(|\langle v, X \rangle| > x)$ for all $v \in \mathcal{S}^{d-1}$. If ν is not an integer and f is a bilipschitz function, then $f(X)$ is tail-isotropic with tail index ν .*

Proof Since $x \mapsto \langle v, f(x) \rangle$ is Lipschitz continuous for any $v \in \mathcal{S}^{d-1}$, Theorem 1.1 implies $\langle v, f(X) \rangle \in \overline{\mathcal{L}}_\nu^1$. Let $\theta \in (0, \pi/2)$ (say, $\theta = \pi/4$), and let $S_v = \{x : \cos^{-1}(\langle x/\|x\|, v \rangle) \leq \theta\}$

for each $v \in \mathcal{S}^{d-1}$. Then

$$H_v := \{x : \langle v, x \rangle > 1\} \supset \{x : \|x\| > (1 - \cos \theta)^{-1}\} \cap S_v.$$

From Theorem C.2.1 of Buraczewski et al. [BDM16], since $\nu \notin \mathbb{Z}$, there exists a non-zero measure μ such that

$$\mu(E) = \lim_{x \rightarrow \infty} \frac{\mathbb{P}(x^{-1}X \in E)}{\mathbb{P}(\|X\| > x)},$$

for any Borel set E . Consequently, μ is regularly varying, and so by the spectral representation of regularly varying random vectors (see p. 281 Buraczewski et al. [BDM16]), there exists a measure P such that

$$\lim_{x \rightarrow \infty} \frac{\mathbb{P}(\|X\| > tx, X/\|X\| \in E)}{\mathbb{P}(\|X\| > x)} = t^{-\nu} P(E),$$

for any Borel set E on \mathcal{S}^{d-1} and any $t > 0$. Letting $F_v = \{y/\|y\| : f(y) \in S_v\} \subset \mathcal{S}^{d-1}$ (noting that $P(F_v) > 0$ by assumption), since $m\|x - y\| \leq \|f(x) - f(y)\| \leq M\|x - y\|$ for all x, y ,

$$\begin{aligned} \liminf_{x \rightarrow \infty} \frac{\mathbb{P}(f(X) \in xH_v)}{\mathbb{P}(\|f(X)\| > x)} &\geq \liminf_{x \rightarrow \infty} \frac{\mathbb{P}(\|f(X)\| > x(1 - \cos \theta)^{-1}, f(X) \in S_v)}{\mathbb{P}(\|f(X)\| > x)} \\ &\geq \liminf_{x \rightarrow \infty} \frac{\mathbb{P}(\|X\| > x(m(1 - \cos \theta))^{-1}, X/\|X\| \in F_v)}{\|X\| > x/M} \\ &\geq P(F_v) \left(\frac{M}{m(1 - \cos \theta)} \right)^{-\nu} > 0, \text{ y.a.B} \end{aligned}$$

where $P(F_v) > 0$ follows from the bilipschitz condition for f . Therefore, we have shown that $\mathbb{P}(\langle v, f(X) \rangle > x) = \Theta(\mathbb{P}(\|f(X)\| > x))$ for every $v \in \mathcal{S}^{d-1}$. Since $\mathbb{P}(\|f(X)\| > x)$ obeys a power law with exponent ν by Corollary 1.1, $f(X)$ is tail-isotropic with exponent ν . ■

Anisotropic tail adaptive flows

To work around this limitation without relaxing Assumption 1.1, it is evident that tail-anisotropic base distributions μ must be considered. Perhaps the most straightforward modification to incorporate a tail-anisotropic base distribution replaces TAF's isotropic base distribution $\prod_{i=1}^d \text{StudentT}(\nu)$ with $\prod_{i=1}^d \text{StudentT}(\nu_i)$. Note that ν is no longer shared across dimensions, enabling d different tail parameters to be represented:

Definition 1.5 *Anisotropic Tail-Adaptive Flows (ATAF) comprise the variational family $\mathcal{Q}_{ATAF} := \{(f \circ \Phi_{Flow})_* \mu_\nu\}$, where $\mu_\nu = \prod_{i=1}^d \text{StudentT}(\nu_i)$, each ν_i is distinct, and f is a bijection between constrained supports [Kuc+17]. Analogous to Jaini et al. [Jai+20], ATAF's implementation treats ν_i identically to the other parameters in the flow and jointly optimizes over them.*

Remark 1.1 *Anisotropic tail-adaptive flows can represent tail-anisotropic distributions with up to d different tail parameters while simultaneously satisfying Assumption 1.1. For example, if $\Phi_{\text{Flow}} = \text{Identity}$ and $\mu_\nu = \prod_{i=1}^d \text{StudentT}(i)$ then the pushforward $(\Phi_{\text{Flow}})_* \mu_\nu = \mu_\nu$ is tail-anisotropic.*

Naturally, there are other parameterizations of the tail parameters ν_i that may be more effective depending on the application. For example, in high dimensions, one might prefer not to allow for d unique indices, but perhaps only fewer. On the other hand, by using only d tail parameters, an approximation error will necessarily be incurred when more than d different tail parameters are present. Figure 1.2 presents a worst-case scenario where the target distribution has a continuum of tail parameters. In theory, this density could itself be used as an underlying base distribution, although we have not found this to be a good option in practice. The key takeaway is that to capture several different tails in the target density, one must consider a base distribution that incorporates sufficiently many *distinct* tail parameters.

Concerning the choice of StudentT families, we remark that since $\text{StudentT}(\nu) \Rightarrow \mathcal{N}(0, 1)$ as $\nu \rightarrow \infty$, ATAF should still provide reasonably good approximations to target distributions in $\overline{\mathcal{E}^2}$ by taking ν sufficiently large.

1.4 Experiments

Here we validate ATAF’s ability to improve a range of probabilistic modeling tasks. Prior work [Jai+20] demonstrated improved density modelling when fat tails are considered, and our experiments are complementary by evaluating TAFs and ATAFs for variational inference tasks as well as by demonstrating the effect of tail-anisotropy for modelling real-world financial returns and insurance claims datasets. We implement using the `beanmachine` probabilistic programming language [Teh+20] and the `flowtorch` library for normalizing flows [Flo21], and we have open-sourced code for reproducing experiments in Supplementary Materials.

All experiments were performed on an Intel i8700K with 32GB RAM and a NVIDIA GTX 1080 running PyTorch 1.9.0 / Python 3.8.5 / CUDA 11.2 / Ubuntu Linux 20.04 via Windows Subsystem for Linux.

Toy Examples

Normal-normal Conjugate Model

We consider a Normal-Normal conjugate inference problem where the posterior is known to be a Normal distribution as well. Here, we aim to show that ATAF performs no worse than ADVI because $\text{StudentT}(\nu) \rightarrow \mathcal{N}(0, 1)$ as $\nu \rightarrow \infty$. Figure 1.4 shows the resulting density approximation, which can be seen to be reasonable for both a Normal base distribution (the “correct” one) and a StudentT base distribution. This suggests that mis-specification (i.e., heavier tails in the base distribution than the target) may not be too problematic.

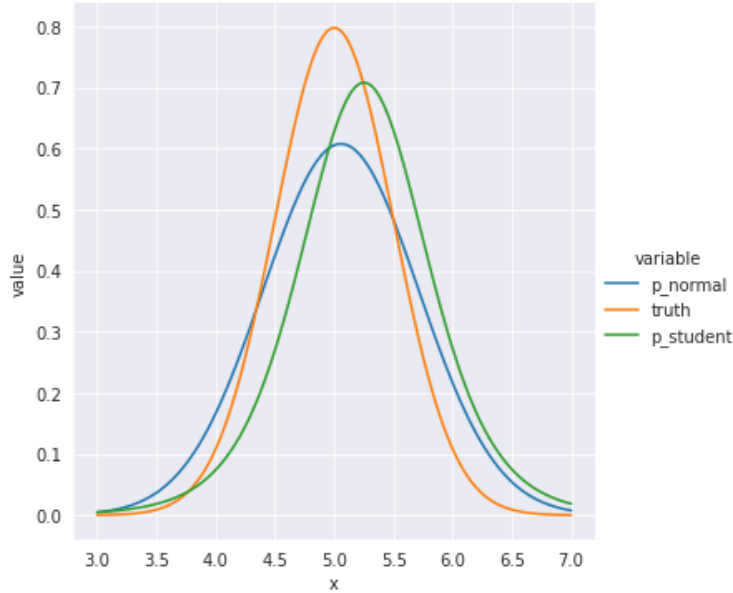


Figure 1.4: Variational inference against a light tailed Normal posterior. Both light and heavy tail variational families yield similar results.

1.5 Experiments Performing VI Against a Fat-tailed Cauchy Target

The motivation for the fat-tailed variational families used in TAF/ATAF is easily illustrated on a toy example consisting of $X \sim \text{Cauchy}(x_0 = 0, \gamma = 1) \in \mathcal{L}_1^1$. As seen in Figure 1.5, while ADVI with normalizing flows [Kin+16; Web+19] appears to provide a reasonable fit to the bulk of the target distribution (left panel), the improper imposition of sub-Gaussian tails results in an exponentially bad tail approximation (middle panel). As a result, samples drawn from the variational approximation fail a Kolmogorov-Smirnov goodness-of-fit test against the true target distribution much more often (right panel, smaller p -values imply more rejections) than a variational approximation which permits fat-tails. This example is a special case of Theorem 1.1.

Real-World Datasets

For all flow-transforms Φ_{Flow} , we used inverse autoregressive flows [Kin+16] with a dense autoregressive conditioner consisting of two layers of either 32 or 256 hidden units depending on problem (see code for details) and ELU activation functions. As described in Jaini et al. [Jai+20], TAF is trained by including ν within the Adam optimizer alongside other flow parameters. For ATAF, we include all ν_i within the optimizer. Models were trained using

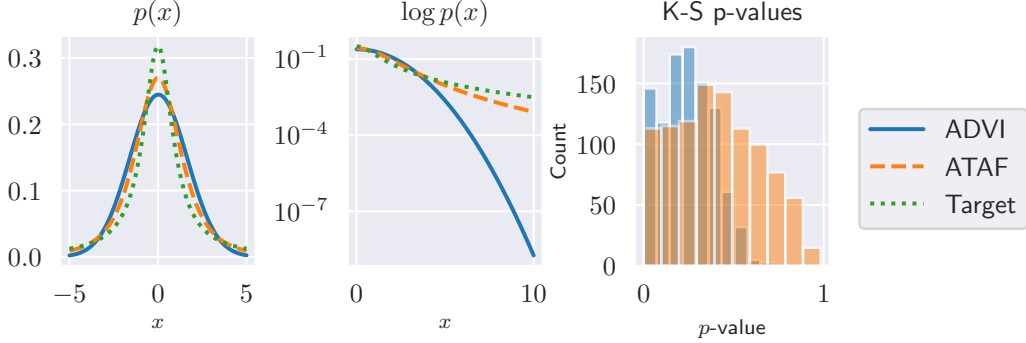


Figure 1.5: When performing FTVI to approximate a $X \sim \text{Cauchy}(x_0 = 0, \gamma = 1)$ target (left panel, green dotted line), the use of a Gaussian variational family (ADVI, solid blue line) can incur exponentially bad tail approximations (middle panel) compared to methods such as ATAF which permit heavier tails (orange dashed line). As a consequence, ADVI samples (blue, right panel) are rejected by the Kolmogorov-Smirnov test more often than ATAF samples (orange, right panel).

the Adam optimizer with 10^{-3} learning rate for 10000 iterations, which we found empirically in all our experiments to result in negligible change in ELBO at the end of training.

For table 1.2a and table 1.2b, the flow transform Φ_{Flow} used for ADVI, TAF, and ATAF is comprised of two hidden layers of 32 units each. NUTS uses no such flow transform. Variational parameters for each normalizing flow were initialized using `torch`’s default Kaiming initialization [He+15]. Additionally, the tail parameters ν_i used in ATAF were initialized to all be equal to the tail parameters learned from training TAF. We empirically observed this resulted in more stable results (less variation in ELBO / $\log p(y)$ across trials), which may be due to the absence of outliers when using a Gaussian base distribution resulting in more stable ELBO gradients. This suggests other techniques for handling outliers such as winsorization may also be helpful, and we leave further investigation for future work.

For fig. 1.6, the closed-form posterior was computed over a finite element grid to produce the “Target” row. A similar progressive training scheme used for table 1.2a was also used here, with the TAF flow transform Φ_{Flow} initialized from the result of ADVI and ATAF additionally initialized all tail parameters ν_i based on the final shared tail parameter obtained from TAF training. Tails are computed along the $\beta = 1$ or $\sigma = 1$ axes because the posterior is identically zero for $\sigma = 0$, hence it reveals no information about the tails.

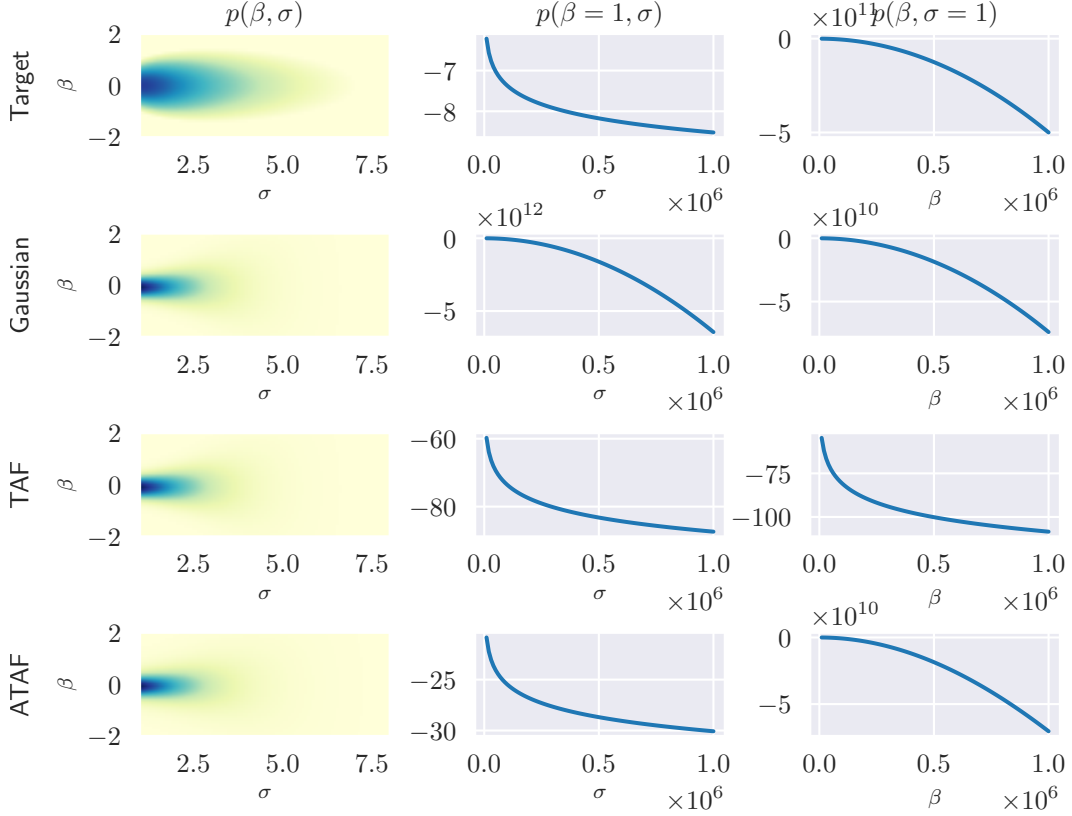


Figure 1.6: Bayesian linear regression’s tail-anisotropic posterior (top left) exhibits a fat-tailed conditional in σ (as evidenced by the convex power-law decay in the top middle panel) and a Gaussian conditional in β (concave graph in top right panel). While all methods appear to provide a good approximation of the bulk (left column), Proposition 1.1 implies Gaussian (Gaussian, second row) or isotropic StudentT product (TAF, third row) base distributions yield Gaussian or power-law tails, respectively, for *both* σ and β . In contrast, ATAF (bottom row) illustrates Remark 1.1 by modeling simultaneously a power-law tail on σ and Gaussian tail on β .

	ELBO	$\log p(y)$		ELBO	$\log p(y)$
ADVI	2873.90 ± 6.95	2969.73 ± 1.73	ADVI	-72.13 ± 6.89	-53.25 ± 3.44
TAF	2839.64 ± 9.10	2973.85 ± 0.87	TAF	-64.64 ± 4.88	-52.51 ± 4.41
ATAF	2842.75 ± 8.83	2976.75 ± 0.66	ATAF	- 58.63 ± 4.75	- 51.01 ± 3.71
NUTS	n/a	3724.59 ± 0.036	NUTS	n/a	-47.78 ± 0.093

(a) diamonds

(b) Eight schools

Table 1.2: Monte-Carlo ELBO and importance weighted Monte-Carlo marginal likelihood $p(y) = \mathbb{E}_{x \sim q_\theta} \frac{p(x, y)}{q_\theta(x)}$ (higher is better, \pm standard errors) estimates from VI on real-world datasets. To understand the variational approximation gap, we include marginal likelihoods based on “golden samples” from `posteriordb` [The21] computed using No-U-Turn-Sampling (NUTS, Hoffman et al. [HG14] and Carpenter et al. [Car+17]).

	Fama-French 5 Industry Daily	CMS 2008-2010 DE-SynPUF
ADVI	-5.018 ± 0.056	-1.883 ± 0.012
TAF	-4.703 ± 0.023	-1.659 ± 0.004
ATAF	- 4.699 ± 0.024	- 1.603 ± 0.034

Table 1.3: Log-likelihoods (higher is better, \pm standard errors) achieved on density modeling tasks involving financial returns [FF15] and insurance claims [Cen10] data.

Bayesian Linear Regression

Consider one-dimensional Bayesian linear regression (BLR) with conjugate priors, defined by priors and likelihood

$$\sigma^2 \sim \text{Inv-Gamma}(a_0, b_0)$$

$$\beta \mid \sigma^2 \sim \mathcal{N}(0, \sigma^2), \quad y \mid X, \beta, \sigma \sim \mathcal{N}(X\beta, \sigma^2),$$

where a_0, b_0 are hyperparameters and the task is to approximate the posterior distribution $p(\beta, \sigma^2 \mid X, y)$. Owing to conjugacy, the posterior distribution can be explicitly computed. Indeed, $p(\beta, \sigma^2 \mid X, y) = \rho(\sigma^2)\rho(\beta \mid \sigma)$ where $\rho(\beta \mid \sigma) = \mathcal{N}(\Sigma_n(X^\top X \hat{\beta}), \sigma^2 \Sigma_n)$, $\Sigma_n = (X^\top X + \sigma^{-2})^{-1}$, $\hat{\beta} = (X^\top X)^{-1} X^\top y$, and

$$\rho(\sigma^2) = \text{Inv-Gamma}\left(a_0 + \frac{n}{2}, b_0 + \frac{1}{2}(y^\top y - \mu_n^\top \Sigma_n \mu_n)\right).$$

This calculation reveals that the posterior distribution is tail-anisotropic: for fixed c we have that $p(\sigma^2, \beta = c \mid X, y) \propto \rho(\sigma^2) \in \mathcal{L}_{\alpha_n}^1$ as a function of σ (with α_n a function of n) and $p(\sigma^2 = c, \beta \mid X, y) \propto \rho(\beta \mid c) \in \overline{\mathcal{E}}^2$ as a function of β . As a result of Proposition 1.1, we

expect ADVI and TAF to erroneously impose Gaussian and power-law tails respectively for both β and σ^2 as neither method can produce a tail-anisotropic pushforward. This intuition is confirmed in Figure 1.6, where we see that only ATAF is the only method capable of modeling the tail-anisotropy present in the data.

Conducting Bayesian linear regression is among the standard tasks requested of a probabilistic programming language, yet it still displays tail-anisotropy. To accurately capture large quantiles, this tail-anisotropy should not be ignored, necessitating a method such as ATAF.

Diamond Price Prediction Using Non-Conjugate Bayesian Regression

Without conjugacy, the BLR posterior is intractable and there is no reason *a priori* to expect tail-anisotropy. Regardless, this presents a realistic and practical scenario for evaluating ATAF’s ability to improve VI. For this experiment, we consider BLR on the **diamonds** dataset [Wic11] included in **posterior**db [The21]. This dataset contains a covariate matrix $X \in \mathbb{R}^{5000 \times 24}$ consisting of 5000 diamonds each with 24 features as well as an outcome variable $y \in \mathbb{R}^{5000}$ representing each diamond’s price. The probabilistic model for this inference task is specified in Stan code provided by The Stan Developers [The21] and is reproduced here for convenience:

$$\begin{aligned}\alpha &\sim \text{StudentT}(\nu = 3, \text{loc} = 8, \text{scale} = 10) \\ \sigma &\sim \text{HalfStudentT}(\nu = 3, \text{loc} = 0, \text{scale} = 10) \\ \beta &\sim \mathcal{N}(0, \mathbf{I}_{24}), \quad y \sim \mathcal{N}(\alpha + X\beta, \sigma).\end{aligned}$$

For each VI method, we performed 100 trials each consisting of 5000 descent steps on the Monte-Carlo ELBO estimated using 1000 samples and report the results in Table 1.2a. We report both the final Monte-Carlo ELBO as well as a Monte-Carlo importance-weighted approximation to the log marginal likelihood $\log p(y) = \log \mathbb{E}_{x \sim q_\theta} \frac{p(x, y)}{q_\theta(y)}$ both estimated using 1000 samples.

Eight Schools SAT Score Modelling with Fat-tailed Scale Mixtures

The eight-schools model [Rub81; Gel+13] is a classical Bayesian hierarchical model used originally to consider the relationship between standardized test scores and coaching programs in place at eight schools. A variation using half Cauchy non-informative priors [Gel+06] provides a real-world inference problem involving fat-tailed distributions, and is formally specified by the probabilistic model

$$\begin{aligned}\tau &\sim \text{HalfCauchy}(\text{loc} = 0, \text{scale} = 5) \\ \mu &\sim \mathcal{N}(0, 5), \quad \theta \sim \mathcal{N}(\mu, \tau), \quad y \sim \mathcal{N}(\theta, \sigma).\end{aligned}$$

Given test scores and standard errors $\{(y_i, \sigma_i)\}_{i=1}^8$, we are interested in the posterior distribution over treatment effects $\theta_1, \dots, \theta_d$. The experimental parameters are identical to Section 1.5, and results are reported in Table 1.2b.

Financial and Actuarial Applications

To examine the advantage of tail-anisotropic modelling in practice, we considered two benchmark datasets from financial (daily log returns for five industry indices during 1926–2021 [FF15]) and actuarial (per-patient inpatient and outpatient cumulative Medicare/Medicaid (CMS) claims during 2008–2010 [Cen10]) applications where practitioners actively seek to model fat-tails and account for black-swan events. Identical flow architectures and optimizers were used in both cases, with log-likelihoods presented in Table 1.3. Both datasets exhibited superior fits after allowing for heavier tails, with a further improved fit using ATAF for the CMS claims dataset.

1.6 Conclusion

In this work, we have sharpened existing theory for approximating fat-tailed distributions with normalizing flows, and we formalized tail-(an)isotropy through a direction-dependent tail parameter. With this, we have shown that many prior flow-based methods are inherently limited by tail-isotropy. With this in mind, we proposed a simple flow-based method capable of modeling tail-anisotropic targets. As we have seen, anisotropic FTVI is already applicable in fairly elementary examples such as Bayesian linear regression; and ATAFs provide one of the first methods for using the representational capacity of flow-based methods, while simultaneously producing tail-anisotropic distributions. A number of open problems still remain, including the study of other parameterizations of the tail behaviour of the base distribution. Even so, going forward, it seems prudent that density estimators, especially those used in black-box settings, consider accounting for tail-anisotropy using a method such as ATAF.

Bibliography

- [AO20] Najmeh Abiri and Mattias Ohlsson. “Variational auto-encoders with Student’s t-prior”. In: *arXiv preprint arXiv:2004.02581* (2020).
- [ASD20] Abhinav Agrawal, Daniel R Sheldon, and Justin Domke. “Advances in black-box VI: Normalizing flows, importance weighting, and optimization”. In: *Advances in Neural Information Processing Systems* 33 (2020), pp. 17358–17369.
- [BDM16] Dariusz Buraczewski, Ewa Damek, and Thomas Mikosch. “Stochastic models with power-law tails”. In: *Springer Ser. Oper. Res. Financ. Eng., Springer, Cham* 10 (2016), pp. 978–3.
- [Bin+19] Eli Bingham, Jonathan P Chen, Martin Jankowiak, Fritz Obermeyer, Neeraj Pradhan, Theofanis Karaletsos, Rohit Singh, Paul Szerlip, Paul Horsfall, and Noah D Goodman. “Pyro: Deep universal probabilistic programming”. In: *The Journal of Machine Learning Research* 20.1 (2019), pp. 973–978.
- [Boe+20] Benedikt Boenninghoff, Steffen Zeiler, Robert M Nickel, and Dorothea Kolossa. “Variational Autoencoder with Embedded Student-*t* Mixture Model for Authorship Attribution”. In: *arXiv preprint arXiv:2005.13930* (2020).
- [Cao+22] Shichen Cao, Jingjing Li, Kenric P Nelson, and Mark A Kon. “Coupled VAE: Improved accuracy and robustness of a variational autoencoder”. In: *Entropy* 24.3 (2022), p. 423.
- [Car+17] Bob Carpenter, Andrew Gelman, Matthew D Hoffman, Daniel Lee, Ben Goodrich, Michael Betancourt, Marcus Brubaker, Jiqiang Guo, Peter Li, and Allen Riddell. “Stan: A probabilistic programming language”. In: *Journal of statistical software* 76.1 (2017).
- [Cen10] Centers for Medicare and Medicaid Services. *CMS 2008-2010 Data Entrepreneurs’ Synthetic Public Use File (DE-SynPUF)*. [Online; accessed 10-March-2020]. 2010. URL: https://www.cms.gov/Research-Statistics-Data-and-Systems/Downloadable-Public-Use-Files/SynPUFs/DE_Syn_PUF.
- [Che+19] Ricky TQ Chen, Jens Behrmann, David K Duvenaud, and Jörn-Henrik Jacobsen. “Residual flows for invertible generative modeling”. In: *Advances in Neural Information Processing Systems* 32 (2019), pp. 9913–9923.

- [CSN20] Kevin R Chen, Daniel Svoboda, and Kenric P Nelson. “Use of Student’s t-Distribution for the Latent Layer in a Coupled Variational Autoencoder”. In: *arXiv preprint arXiv:2011.10879* (2020).
- [DKB15] L Dinh, D Krueger, and Y Bengio. “NICE: non-linear independent components estimation”. In: *3rd International Conference on Learning Representations, Workshop Track Proceedings*. 2015.
- [DQV11] Nan Ding, Yuan Qi, and Svn Vishwanathan. “t-divergence based approximate inference”. In: *Advances in Neural Information Processing Systems* 24 (2011), pp. 1494–1502.
- [DSB17] Laurent Dinh, Jascha Sohl-Dickstein, and Samy Bengio. “Density estimation using Real NVP”. In: *5th International Conference on Learning Representations*. 2017.
- [Dur+19] Conor Durkan, Artur Bekasov, Iain Murray, and George Papamakarios. “Neural spline flows”. In: *Advances in Neural Information Processing Systems* 32 (2019), pp. 7509–7520.
- [FF15] Eugene F Fama and Kenneth R French. “A five-factor asset pricing model”. In: *Journal of Financial Economics* 116.1 (2015), pp. 1–22.
- [Flo21] FlowTorch Development Team. *Flowtorch*. [Online; accessed 15-May-2021]. 2021. URL: <https://flowtorch.ai/>.
- [FSS17] Futoshi Futami, Issei Sato, and Masashi Sugiyama. “Expectation propagation for t-exponential family using q-algebra”. In: *Advances in Neural Information Processing Systems* 30 (2017), pp. 2245–2254.
- [Gel+06] Andrew Gelman et al. “Prior distributions for variance parameters in hierarchical models (comment on article by Browne and Draper)”. In: *Bayesian analysis* 1.3 (2006), pp. 515–534.
- [Gel+13] Andrew Gelman, John B Carlin, Hal S Stern, David B Dunson, Aki Vehtari, and Donald B Rubin. *Bayesian data analysis*. CRC press, 2013.
- [GH06] Andrew Gelman and Jennifer Hill. *Data analysis using regression and multi-level/hierarchical models*. Cambridge university press, 2006.
- [Gra+19] Will Grathwohl, Ricky T. Q. Chen, Jesse Bettencourt, Ilya Sutskever, and David Duvenaud. “FFJORD: Free-Form Continuous Dynamics for Scalable Reversible Generative Models”. In: *International Conference on Learning Representations*. 2019.
- [He+15] Kaiming He, Xiangyu Zhang, Shaoqing Ren, and Jian Sun. “Delving deep into rectifiers: Surpassing human-level performance on imagenet classification”. In: *Proceedings of the IEEE international conference on computer vision*. 2015, pp. 1026–1034.

- [HG14] Matthew D Hoffman and Andrew Gelman. “The No-U-Turn sampler: adaptively setting path lengths in Hamiltonian Monte Carlo.” In: *J. Mach. Learn. Res.* 15.1 (2014), pp. 1593–1623.
- [Hua+18] Chin-Wei Huang, David Krueger, Alexandre Lacoste, and Aaron Courville. “Neural autoregressive flows”. In: *International Conference on Machine Learning*. PMLR. 2018, pp. 2078–2087.
- [Hus17] Ferenc Huszár. “Variational inference using implicit distributions”. In: *arXiv preprint arXiv:1702.08235* (2017).
- [Jai+20] Priyank Jaini, Ivan Kobyzev, Yaoliang Yu, and Marcus Brubaker. “Tails of Lipschitz Triangular Flows”. In: *International Conference on Machine Learning*. PMLR. 2020, pp. 4673–4681.
- [JSY19] Priyank Jaini, Kira A Selby, and Yaoliang Yu. “Sum-of-squares polynomial flow”. In: *International Conference on Machine Learning*. PMLR. 2019, pp. 3009–3018.
- [KD18] Diederik Kingma and Prafulla Dhariwal. “Glow: Generative Flow with Invertible 1x1 Convolutions”. In: *Advances in Neural Information Processing Systems* 31 (2018), pp. 10236–10245.
- [Kin+16] Durk P Kingma, Tim Salimans, Rafal Jozefowicz, Xi Chen, Ilya Sutskever, and Max Welling. “Improved variational inference with inverse autoregressive flow”. In: *Advances in neural information processing systems*. 2016, pp. 4743–4751.
- [Kuc+17] Alp Kucukelbir, Dustin Tran, Rajesh Ranganath, Andrew Gelman, and David M Blei. “Automatic differentiation variational inference”. In: *The Journal of Machine Learning Research* 18.1 (2017), pp. 430–474.
- [Led01] Michel Ledoux. *The concentration of measure phenomenon*. Mathematical surveys and monographs 89. American Mathematical Soc., 2001.
- [LHM22] Feynman Liang, Liam Hodgkinson, and Michael Mahoney. “Fat-Tailed Variational Inference with Anisotropic Tail Adaptive Flows”. In: *Proceedings of the 39th International Conference on Machine Learning*. Vol. 162. 2022, p. 132.
- [LT16] Yingzhen Li and Richard E Turner. “Rényi divergence variational inference”. In: *Advances in Neural Information Processing Systems* 29 (2016), pp. 1073–1081.
- [Mat+19] Emile Mathieu, Tom Rainforth, N Siddharth, and Yee Whye Teh. “Disentangling disentanglement in variational autoencoders”. In: *International Conference on Machine Learning*. PMLR. 2019, pp. 4402–4412.
- [Pap+21] George Papamakarios, Eric Nalisnick, Danilo Jimenez Rezende, Shakir Mohamed, and Balaji Lakshminarayanan. “Normalizing flows for probabilistic modeling and inference”. In: *Journal of Machine Learning Research* 22.57 (2021), pp. 1–64.
- [PHF10] Anand Patil, David Huard, and Christopher J Fonnesbeck. “PyMC: Bayesian stochastic modelling in Python”. In: *Journal of Statistical Software* 35.4 (2010), p. 1.

- [PPM17] George Papamakarios, Theo Pavlakou, and Iain Murray. “Masked autoregressive flow for density estimation”. In: *Advances in Neural Information Processing Systems*. 2017, pp. 2338–2347.
- [RGB14] Rajesh Ranganath, Sean Gerrish, and David Blei. “Black box variational inference”. In: *International Conference on Artificial Intelligence and Statistics*. PMLR. 2014, pp. 814–822.
- [RM15] Danilo Rezende and Shakir Mohamed. “Variational inference with normalizing flows”. In: *International Conference on Machine Learning*. PMLR. 2015, pp. 1530–1538.
- [Rub81] Donald B Rubin. “Estimation in parallel randomized experiments”. In: *Journal of Educational Statistics* 6.4 (1981), pp. 377–401.
- [Teh+20] Nazanin Tehrani, Nimar S Arora, Yucen Lily Li, Kinjal Divesh Shah, David Noursi, Michael Tingley, Narjes Torabi, Eric Lippert, Erik Meijer, et al. “Bean machine: A declarative probabilistic programming language for efficient programmable inference”. In: *International Conference on Probabilistic Graphical Models*. PMLR. 2020.
- [The21] The Stan Developers. *posteriordb: a database of Bayesian posterior inference*. <https://github.com/stan-dev/posteriordb>. 2021.
- [TL05] Michael E Tipping and Neil D Lawrence. “Variational inference for Student-t models: Robust Bayesian interpolation and generalised component analysis”. In: *Neurocomputing* 69.1-3 (2005), pp. 123–141.
- [Web+19] Stefan Webb, J.P. Chen, Martin Jankowiak, and Noah Goodman. “Improving Automated Variational Inference with Normalizing Flows”. In: *6th ICML Workshop on Automated Machine Learning (AutoML)* (2019).
- [Wic11] Hadley Wickham. “ggplot2”. In: *Wiley Interdisciplinary Reviews: Computational Statistics* 3.2 (2011), pp. 180–185.
- [WL19] Antoine Wehenkel and Gilles Louppe. “Unconstrained monotonic neural networks”. In: *Advances in Neural Information Processing Systems* 32 (2019), pp. 1543–1553.
- [WLL18] Dilin Wang, Hao Liu, and Qiang Liu. “Variational inference with tail-adaptive f-divergence”. In: *Advances in Neural Information Processing Systems* 31 (2018), pp. 5737–5747.
- [WW13] David Wingate and Theophane Weber. “Automated variational inference in probabilistic programming”. In: *arXiv preprint arXiv:1301.1299* (2013).